

Lawrence Berkeley National Laboratory

LBL Publications

Title

A novel all-solid electrolyte based on a co-polymer of poly-(methoxy/hexadecal-poly(ethylene glycol) methacrylate) for lithium-ion cell

Permalink

<https://escholarship.org/uc/item/8933m4bh>

Journal

Journal of Materials Chemistry, 22(41)

ISSN

0959-9428

Authors

Zuo, Xiang
Liu, Xiao-Min
Cai, Feng
et al.

Publication Date

2012

DOI

10.1039/c2jm34270g

Peer reviewed

A Novel All-Solid Electrolyte Based on Co-polymer of Poly-(Methoxy/Hexadecyl-Poly(Ethylene Glycol) Methacrylate) for Lithium-ion Cell

Xiang Zuo^a, Xiao-Min Liu^a, Feng Cai^a, Hui Yang^a, Xiao-Dong Shen^a and Gao Liu^b

^a College of Materials Science and Engineering, Nanjing University of Technology, 5

Xinmofan Road, Nanjing, Jiangsu, 210009, P. R. China

^b Environmental Energy Technologies Division, Lawrence Berkeley National Laboratory, 1

Cyclotron Rd., Berkeley, CA, 94720, USA

Abstract

A novel comb-like copolymer solid electrolyte with a relatively high ionic conductivity, $10^{-3.9} \text{ S}\cdot\text{cm}^{-1}$ at 30°C and $10^{-3.1} \text{ S}\cdot\text{cm}^{-1}$ at 80 °C, is prepared by free radical polymerization in this study. The polymer consists of methacrylate as backbone and a mixture of hexadecyl (C_{16})/methoxyl terminated oligo(ethylene oxide) at a certain ratio as side chains. Fourier transform infrared spectroscopy (FTIR) and differential scanning calorimetry (DSC) analysis reveal that non-polar unit (C_{16}) end-modification not only greatly increases the mobility of the ethylene oxide (EO) chains, but also suppresses their local crystallization behavior by interrupting the regular arrangement, therefore improving the conductivity of the obtained electrolyte.

Keywords: Comb-like copolymer; Non-polar; End-modification; Polymer Electrolyte; Lithium-ion Cell

1. Introduction

Solid polymer electrolyte (SPE) is a candidate for traditional liquid electrolyte in lithium-ion cells with improved reliability and safety. It has been extensively studied for more than 20 years and most of the research work focused on poly(ethylene oxide) (PEO) and its derivatives as a matrix polymer due to its ability to dissolve salts and its high segmental flexibility for ion transport in amorphous phase [1-3]. However, the linear PEO of high molecular weight exhibits fairly low ionic conductivity ($10^{-7}\sim 10^{-8} \text{ S}\cdot\text{cm}^{-1}$) due to its crystallization propensity at temperatures lower than 65°C. Several research groups [4-6] reported that the comb-like polymer electrolytes with more flexible oligomeric PEO side chains exhibits higher ion conduction ($10^{-5}\sim 10^{-6} \text{ S}\cdot\text{cm}^{-1}$) at ambient temperatures. The introduction of polar units (amide [7], nitrile [8,9], maleic anhydride [10] and fluorine [11], etc.) into the main or side chains, which can provide high concentration of charge carriers due to the significant ionization of the lithium salt, is a common method to further improve both ionic conductivity and mechanical stability in many recent studies. Higa et al. [7] synthesized a graft copolymer electrolyte with a relatively high conductivity ($10^{-5.18} \text{ S}\cdot\text{cm}^{-1}$ at 25°C) and excellent tensile strength (100MPa) which contains a polyimide main chain and methoxy-poly(ethylene glycol) methacrylate side chains. Lee et al. [10] prepared a comb-like polymer electrolyte with cross-linked structure based on maleic anhydride and PEO which can be applied in high temperature application since it exhibits a conductivity up to $10^{-4} \text{ S}\cdot\text{cm}^{-1}$ at 90°C. Since the strong Van der Waals forces between the EO units and the polar units may hinder the motion of the EO chains, the introduction of non-polar units might circumvent the Van der Waals force to further improve the conductivity. Patric [12,13] presented a novel polymer system that all grafts were copolymerized by a mixture of ethylene oxide (EO)/propylene oxide (PO) and ended with non-polar units. It was claimed that PO chains defect the crystallinity of EO chains by disrupting the regular structure and the non-polar units act as “physical cross-linker” to improve the dimensional stability. Hence, the presence of PO chains and non-polar units improve the conductivity to $10^{-4.25} \text{ S}\cdot\text{cm}^{-1}$ at 30 °C and $10^{-3.2} \text{ S}\cdot\text{cm}^{-1}$ at 80 °C. The conductance improvement of the above system is limited by the low conductivity of PO units and the crystallization of the EO units which cannot be eliminated completely due to the existence of long-chain of EO/PO ($\sim 2000 \text{ g}\cdot\text{mol}^{-1}$).

In this study, a novel comb-like polymer was designed by co-polymerizing of two

macro-monomers: methoxy-poly(ethylene glycol) methacrylate (MPEGM, $n=7, 12, 16$) and hexadecyl-poly(ethylene glycol) methacrylate (HPEGM, $n=7$) (Fig. 1). As illustrated in Fig. 2, the regular arrangement of the EO chains (Fig. 2a) and hydrocarbons C_{16} (Fig. 2b) could result in local crystallization in Poly-MPEGM and Poly-HPEGM, respectively. While the regular arrangements of both EO chains and hydrocarbons are disrupted in poly(MPEGM-co-HPEGM) shown in Fig. 2c, the local crystallization may be eliminated completely. The introduction of the C_{16} end-modification into some grafts expands the free volume of main chains and side chains, weakens the interaction between the adjacent macromolecules as well as the adjacent polar EO units. The expanding free volume of the EO chains and the improved flexibility of the main chains are beneficial to the ion conduction within the synthesized polymer electrolyte.

2. Experimental

2.1 Materials

Methoxy-poly(ethylene glycol) (MPEG350, 550, 750, $n = 7, 12, 16$) and hexadecyl-poly(ethylene glycol) (HPEG578, $n=7$), obtained from Alfa Aesar and TCI, respectively, were stored over 4 Å molecular sieves to remove residual moisture before use. Triethylamine (TEA), and methacryloyl chloride, were used as received from Aladdin. The lithium salt, LiClO_4 (99.9%, Aladdin) was dried under reduced pressure at 120 °C for 24 hrs before use.

2.2 Synthesis of methoxy-poly(ethylene glycol) methacrylate (MPEGM)

Methoxy-poly(ethylene glycol) methacrylates ($n=7, 12, 16$) were prepared by using methacryloyl chloride to esterificate the terminal hydroxyl groups of methoxy-poly(ethylene glycol) (MPEG350, 550, 750). A well stirred mixture of 0.10 mol MPEG, 0.12 mol TEA and 250mL dry dichloromethane (DCM) was cooled to 0 °C in an ice-water bath. Methacryloyl chloride (0.12 mol) was added dropwise to the above mixture followed by 12 hour stir. The crude product, obtained after filtration and vacuum evaporation, was purified by silica gel column with petroleum aether and ethyl acetate (volume ratio of 5:1) as eluent. A pale yellow product MPEGM was obtained after vacuum desolventizing.

2.3 Synthesis of hexadecyl-poly(ethylene glycol) methacrylate (HPEGM)

HPEGM was prepared in a similar method to MPEGM with the following reagents: hexadecyl-poly(ethylene glycol) (HPEG578, 0.1mol), triethylamine (0.12mol), and methacryloyl chloride (0.12 mol). The final product purified by silica gel column was isolated as a yellow oily liquid.

2.4 Synthesis of Poly(MPEGM-co-HPEGM)

A homogeneous solution was prepared by dissolving certain amounts of MPEGM and HPEGM monomers in anhydrous N, N-dimethylformamide (DMF) with 2,2-azobisisobutyronitrile (AIBN) as the initiator (5wt% of total monomers mass). After 6~8 hours polymerization process at 60 °C under nitrogen atmosphere, the obtained viscous liquid was transferred into a large excess of de-ionized water, then washed by deionized water for three times. Afterwards, the co-polymer was dried at 100 °C under vacuum till the weight did not change. The random graft Poly(MPEGM-co-HPEGM) was characterized by ^{13}C -NMR and IR spectra.

For convenience, poly(MPEGM-co-HPEGM) prepared at different mass ratios of MPEGM and HPEGM was abbreviated as the followings: the copolymer prepared by MPEGM (n=7) and HPEGM at the weight ratio of 80:20 was abbreviated as PMH₇-20.

2.5 Preparation of the polymer electrolyte

The mixture of LiClO₄ and copolymer at a desired [Li]:[EO] ratio in anhydrous DMF, was cast in Teflon molds and evaporated under Argon for 2 days at room temperature. Then, the obtained electrolyte films were dried at 80 °C under high vacuum for 72 hours to remove the solvent residue.

2.6 Material Characterization and Conductivity Measurement

IR spectra were recorded using a TENSOR 27 Fourier transform spectrometer over the range of 4000-400cm⁻¹ at 25°C. ¹H NMR spectra of the samples were obtained from a 500 MHz BRUKE NMR spectrometer in chloroform-d. The chemical shifts for ¹H-NMR measurements were referred to tetramethylsilane (TMS) as internal standard. ¹³C NMR spectra were recorded with the same spectrometer in DMSO-d₆.

Thermal analysis was conducted with a DSC200F3 (NETZSCH) differential scanning calorimeter over the temperature range of -100°C ~100°C under N₂ atmosphere at the scan rate of 10°C •min⁻¹. The sample, placed in the aluminum containers, was first heated to 100°C, then cooled down to -100°C and scanned. Thermogravimetric analysis (TGA) was conducted under nitrogen environment at the heating rate of 10 °C•min⁻¹ from 25 °C to 500 °C by a TA instrument STA409PC (NETZSCH).

The ionic conductivity of the samples was measured by alternating current (A. C.) impedance spectroscopy using an impedance analyzer (PARSTAT 2273) in the frequency range of 0.1 Hz to 1MHz. The polymer electrolyte was sandwiched by two polished stainless-steel electrodes, sealed in a testing cell within an Argon-housed dry box. Then the testing cell was measured in the temperature range from 10 °C to 80 °C. The electrochemical stability of the electrolyte was determined by cyclic voltammetry (CV) scans using a nickel plate (Ni) as the working electrode and lithium as the counter and reference electrodes. The CV scans were performed at the scan rate of 5 mV•s⁻¹ from -0.5 V to 2.5 V vs. Li⁺/Li and from 2.5V to 5.5 V vs. Li⁺/Li at 30 °C, respectively. The interfacial resistance between electrolyte and lithium electrode was analyzed by A. C. impedance spectroscopy using PARSTAT 2273 impedance analyzer for a Li/SPE/ Li cell.

3. Results and Discussion

3.1 ^{13}C -NMR: determination of the copolymer structure

Fig. 3 illustrates the ^{13}C -NMR spectra of PMH₇₋₈₀ and the assigned chemical shifts of various carbon resonances. The resonance peaks at 176.41, 69.80, 57.97 and 39.22 ppm are assigned to the carbonyl carbons, ether carbons of PEG, methoxyl carbons and carbons of C₁₆, respectively. The disappearance of the double bond carbon resonance peaks ranging 130-124 ppm indicates that the PMH₇₋₈₀ was successfully synthesized by copolymerizing MPEGM (n=7) and HPEGM.

3.2 FTIR analysis

3.2.1 Copolymer structure

Fig. 4 presents the IR spectra of MPEGM (n=7), HPEGM and PMH₇₋₈₀. Fig. 4(a) shows the characteristic absorption peaks of the MPEGM monomer at 2873 cm⁻¹ (C-H in EO chains), 1729cm⁻¹ (C=O), 1644cm⁻¹ (C=C), and 1107cm⁻¹ (C-O-C). The end methoxy group in MPEGM is substituted by hexadecyl group in HPGEM when the large broad peak at 2873 cm⁻¹ splits into two peaks (Fig. 4(b)) since the local environment of C-H bond in C₁₆ is different from that in EO chains. Comparing the IR spectrum of the copolymer (Fig. 4(c)) with those of the monomers, it can be found that the absorption peaks of C-H, C=O and C-O-C do not change during the copolymerization, but the absorption peak at 1644 or 1638 cm⁻¹ for C=C disappears, indicating that 1) the copolymer maintains the main characteristics of the monomers; 2) the monomers are co-polymerized through the break of double carbon bonds in both MPEGM (n=7) and HPEGM.

3.2.2 The effect of end-modification by C₁₆

EO chains in the PEO macromolecules aggregate regularly and tend to crystallize at ambient temperature due to the highly regular structure and the strong Van der Waals force between the polar C-O-C groups. Therefore, the motion of EO chains is restrained which hinders the lithium ion conduction, especially at ambient condition. In order to improve the ionic conductivity, a type of polymer with loose EO chain packing structure is synthesized by employing bulky hydrocarbon end-modification. The reasons to introduce hydrocarbon chains are as followings: First, hydrocarbon chains shield partial Van der Waals force between polar EO chains by the stereo

hindrance effect. Second, hydrocarbon chains having poor compatibility with C-O-C groups reduce the regularity and the entanglement of the EO chains.

IR spectra was used to investigate the specific intermolecular interaction change qualitatively by the intensity, bandwidth and position of the characteristic absorption peaks [9,14-18]. Fig. 5 shows the IR spectra of the polar C-O-C absorption peaks nearby 1100 cm^{-1} of a series of polyethylene glycol derivatives (Tabulated in Table 1). Due to the weakened interaction and loosened packing of EO chains by non-polar hydrocarbon, the stretching vibration of C-O-C group maybe facilitated and its absorption peak shifts to a higher frequency. It can be concluded that the polymer with a larger non-polar terminal group presents a higher C-O-C vibration frequency, which is more convincing when a higher content and/or a larger volume of the end non-polar group is introduced.

The same phenomenon is also observed in polyethylene glycol based macromonomers and polymers presented in Fig. 6. When the end methoxyl group in MPEGM replaced by C_{16} , the characteristic absorption peak of C-O-C frequency shifts from 1110 cm^{-1} to 1120 cm^{-1} . However, when MPEGM and HPEGM are polymerized separately, the absorption peak of C-O-C shifts to 1107 cm^{-1} and 1118 cm^{-1} , respectively. The possible reason for such shift is that the EO chains become compact after polymerization so that the C-O-C vibration is restrained. The C-O-C absorption peaks of PMH₇₋₈₀, PMH₇₋₆₀, PMH₇₋₄₀ are located at 1110 cm^{-1} , 1112 cm^{-1} , 1115 cm^{-1} , respectively, indicating that the mobility of the EO chains in PMH is better than that in PMPEGM.

3.2.3 Interaction between Li^+ and polar groups

The interaction capability of the polar groups (both C=O and C-O-C) in the electrolytes with Li^+ can be characterized by IR spectra. In theory, the absorption behavior of Li^+ bonded C=O and C-O-C groups is similar to that of the hydrogen bonded C=O and C-O-C groups, that is, the peak of the bonded group shifts to a lower wave number because of the reduced electron density [9,14, 19]. Fig. 7 shows the IR spectra of several PMH₇₋₈₀ based electrolytes. The C-O-C absorption peak of each PMH₇₋₈₀ based electrolyte shifts to lower frequency compared to the PMH₇₋₈₀ polymer. In addition, with the increase of the salt concentration, the C-O-C absorption peak shows lower frequency. The peak at 1729 cm^{-1} is assigned to the C=O group of the methacrylate. All carbonyl absorption peaks do not change with the lithium salt concentration. It can be suggested that most of the Li^+ coordinate to the C-O-C group in the studied concentration range

since the C–O–C groups in copolymer is much more than the C=O groups.

3.2 Thermal behaviors

The thermal data of the neat polymers and polymer electrolytes obtained by DSC are summarized in Table 2 and illustrated in Fig. 8. The melting point of PMPEGM increases with the number of repeating EO unit. No EO chain melting peak is observed for PHPEGM, but crystallization occurs at around -8.2 °C due to the crystallization of C₁₆ chain. No melting or crystallization peak is detected in the PMH samples, indicating that PMH based electrolyte may exhibit good conductivity at low temperatures compared to PMPEGM based electrolyte due to the suppressed crystallization of the EO chains. Based on the correlation between T_g and segmental motion of the EO chains: the lower T_g, the higher mobility of the EO chains. PMH shows a lower T_g than PMPEGM for the reason (crystallization tend to enhance T_g of the PEO) that the steric hindrance effect of C₁₆ promotes the motion of the EO chains by expanding the free volume. The electrolytes have a higher T_g than the neat polymers. The possible reason behind is the formed coordination of ether oxygen with Li⁺ as explained in the FTIR part.

3.3 Electrical properties

3.3.1 Effect of lithium salt concentration

Fig. 9 shows the dependence of the ionic conductivity (σ) and T_g on the [Li]:[EO] ratio. The conductivity curves exhibit a typical bell shape with the maximum conductivity at [Li]:[EO] = 1:20 for all three polymer electrolytes. The bell shape curve of the conductivity regarding the lithium salt concentration is routinely observed for PEO-based electrolytes [8,9,10,19] since the conductivity is proportional to the charge carrier density and the mobility of EO chains. When the lithium salt concentration is low, the salt tends to dissociate to increase the lithium ion concentration resulting in the increase of the number of mobile ions and the conductivity. On the other hand, the dissociated Li⁺ above certain amount may form neutral contact ion pairs with ClO₄⁻ leading to the decrease of the conductivity. In addition, the glass transition temperature increases with the [Li]:[EO] ratio, which can be attributed to the inter- and intra-molecular coordination between Li⁺ and EO units, and further decreasing the motion of EO chains. It can be deduced that the various PMH-based electrolytes achieve the best conductivity at [Li]:[EO]=1:20.

3.3.2 Effect of HPEGM content

Fig. 10 shows the conductivity measured by A. C. impedance spectroscopy as a function of

the HPEGM content at 30°C for three co-polymer electrolytes with different repeat units in MPEGM. For all three samples, the conductivity increases with the HPEGM content, up to the maximum when the HPEGM contents is 20%-30%, then decreases with the further increase of the HPEGM content. The sample PMH₁₂-25 exhibits the highest conductivity, 10^{-3.9} S•cm⁻¹, which is relatively high in all-solid polymer electrolytes reported so far. It can be derived that the introduction of the C₁₆ end modification by HPEGM, plays an important role in the conductivity improvement of the co-polymer since the existence of HPEGM could increase the mobility of the grafted EO chains due to more free volume and weaker interaction between the adjacent EO chains. From the other point, such improvement may be limited since the end group C₁₆ in HPEGM is non-conductive. Comparing the three samples, it can be indicated that the conductivity of the copolymer is mainly affected by the number of the repeating EO units in MPEGM. The mobility of the EO chains is influenced by T_g and length of the EO chains. The copolymer with short EO chains shows high T_g, reducing the mobility. On the contrary, the long EO chains is easy to tangle, restraining the mobility. In conclusion, the conductivity of the solid polymer electrolytes can be optimized by adjusting 1) the repeating units of MPEGM, 2) lithium salt concentration and 3) the ratio of the monomers. The best conductivity, 1.26×10⁻⁴ S•cm⁻¹ at 30°C, was achieved for sample PMH₁₂-25 at the salt concentration of [Li]:[EO] = 1:20.

3.3.3 Dependence of ionic conductivity on temperature

The dependence of the conductivity on temperature for the polymer electrolytes based on PMH₉-80, PMH₁₂-75, PMH₁₆-70 and PHPEGM was also studied in the temperature range from 10 °C to 80 °C and plotted in Fig. 11. The curves show slightly positive deviation from the Arrhenius relationship corresponding to a typical Vogel-Tamman-Fulcher (VTF) expression (Eq. 1)

$$\sigma = AT^{-1/2}e^{-E_a/R(T-T_0)} \quad (\text{Eq. 1})$$

where A is the constant proportional to the number of carrier ions, E₀ is the pseudo-activation energy related to the motion of the polymer segment, R is the Boltzmann constant, and T₀ is the reference temperature, normally associated with the ideal T_g at which the free volume is zero or with the temperature at which the configuration entropy becomes zero. According to the Adam-Gibbs analysis, T₀ is usually taken as 50 K below the measured T_g. The fitted parameter, A,

E_0 , and T_0 are summarized in Table 3. The E_0 of the polymer electrolyte is calculated to be 7.26-8.90 kJ/mol and is proportional to the glass transition temperature of electrolyte since a higher mobility of lithium ion can be achieved by the higher degree of freedom for polymer chain movement. The VTF expression implies that the main mechanism of ion conduction is couple to the segmental mobility of the EO chains that was commonly observed in amorphous polymer electrolyte by many researchers[19-21].

3.3.4 Electrochemical stability of polymer electrolytes

In order to study the electrochemical stability of the obtained electrolytes (PMH₇₋₈₀, PMH₁₂₋₇₅, PMH₁₆₋₇₀), cyclic voltammogram scans were performed with Ni as the working electrode and Li as the reference/counter electrodes. The electrochemical windows of the three electrolytes are in the similar range regardless of the difference of EO repeating units as shown in Fig 12(a) and 12(b). The oxidation peak appears at 4.5 V vs. Li⁺/Li, while the reversible lithium plating/stripping takes place in the potential range of -0.5 to 0.5V (versus Li⁺/Li). Therefore, the obtained polymer electrolytes have stable potential window up to 4.5V as well as reversible plating/stripping of Li on the Ni electrode, which could be applied to the practical lithium polymer battery [22-24].

3.3.5 Interface stability between lithium electrode and polymer electrolyte

The interface stability between the lithium and the polymer electrolyte was measured by measuring the A. C. impedance of a Li/ PMO₁₂₋₇₅ based electrolyte/Li cell stored at 30 °C under open-circuit potential condition. Fig. 13(a) and Fig. 13(b) present the Nyquist spectra and the change in the area specific bulk and interface resistances (R_{bulk} and R_{intf}) as a function of storage time. Generally, the interface between the polymer electrolyte and the Li electrode exhibits high resistance up to $10^3 \Omega$ [24,25] due to imperfect contact and the formation of a passivation layer on the Lithium electrode. In this study, R_{bulk} and R_{intf} in the fresh cell are $450 \Omega \cdot \text{cm}^2$ and $950 \Omega \cdot \text{cm}^2$, respectively. R_{bulk} changes little during the storage and stabilizes at around $550 \Omega \cdot \text{cm}^2$. However, R_{intf} shows a progressive increase to a steady value at $1250 \Omega \cdot \text{cm}^2$ after 10 days. The R_{intf} increase may be explained by the formation of a passivation film on the surface of the lithium electrode due to residual impurities in the polymer electrolyte. The impedance results imply that the PMH₁₂₋₇₅ based electrolyte is compatible with the lithium electrode well.

4. Conclusions

A novel comb-like polymer electrolyte was synthesized from MPEGM($n=7, 12, 16$) and HPEGM complexed with LiClO_4 . The ionic conductivity of the polymer electrolyte is related to the numbers of repeating EO units in MPEGM, the weight ratio of the monomers—MPEGM to HPEGM, and lithium salt concentration. The polymer electrolyte prepared with the weight ratio of MPEGM($n=12$) to HPEGM at 75:25 and the ration of Li to EO at 1:20 presents the highest ionic conductivity and good electrochemical compatibility with lithium electrode. (How to justify figure 8) Non-polar unit (C_{16}) end-modification (HPEGM) mobilizes the EO grafts and suppresses the local crystallization by interrupting the regular packing, hence improving the conductivity of the obtained electrolyte. Furthermore, the ion conductivity can be significantly increased by addition of plasticizers such as Polyethylene glycol dimethyl ether, which will be discussed in another paper.

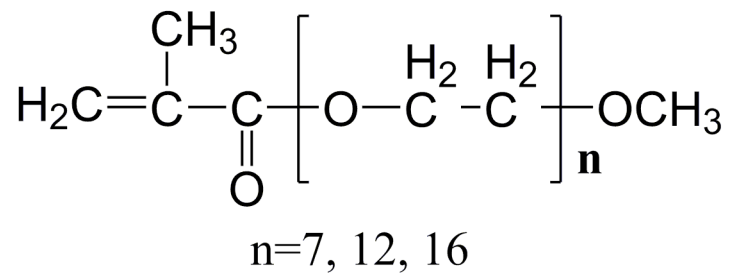
Acknowledgements

This work was supported by Key Project of Natural Science Foundation of Jiangsu Province of China (Grant No. BK2011030), Key Project of Educational Commission of Jiangsu Province of China (Grant No. 11KJA430006) and the Priority Academic Program Development of Jiangsu Higher Education Institutions.

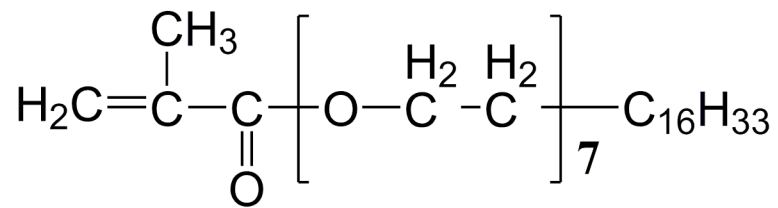
References

- [1] P. Judeinstein, F Roussel, *Adv. Mater.* 17 (2005) 723
- [2] W. H. Meyer, *Adv. Mater.* 10 (1998) 439.
- [3] E. Quartarone, P. Mustarelli, *Chem. Soc. Rev.* 40 (2011) 2525.
- [4] J. F. Snyder, R. H. Carter, E. D. Wetzel. *Chem. Mater.* 19 (2007) 3793.
- [5] N. Yoshimoto, O. Shimamura, T. Nishimura, M. Egashira, M. Nishioka, M. Morita. *Electrochem. Commun.* 11 (2009) 481.
- [6] P. P. Soo, B. Huang, Y. I. Jang, Y. M. Chiang, D. R. Sadoway, A. M. Maye. *J. Electrochem.Soc.* 146 (1999) 32.
- [7] M. Higa, K. Yaguchi, R. Kitani, *Electrochim. Acta* 55 (2010) 1380.
- [8] W. H. Hou, C. Y. Chen, *Electrochim. Acta* 49 (2004) 2105.
- [9] W. H. Hou, C. Y. Chen, C. C. Wang, *Polymer* 44 (2003) 2983.
- [10] S. M. Lee, W. L. Yeh, C. C. Wang, C. Y. Chen, *Electrochim. Acta* 49 (2004) 2667.
- [11] P. Gavelin, R. Ljungbäck, P. Jannasch, B. Wesslen. *Solid State Ionics* 147 (2002) 325.
- [12] P. Jannasch, *Macromolecules* 33 (2000) 8604.
- [13] P. Jannasch, *Electrochim. Acta* 46 (2001) 1641.
- [14] Y. Huang, X. Y Ma, S. H Wang, X. Wang, Y. H Lin. *Ionics* 18 (2012) 167.
- [15] A. Bernson, J. Lindgren. *Polymer* 36 (1995) 4471.
- [16] I. D. Wu, F. C. Chang. *Polymer* 48 (2007) 989.
- [17] R. G. Zhibankov, S. P. Firsov, T. E. Kolosova, L. K. Prihodchenko, D. D. Grinshpan, J. Baran, M. K. Marchewka, H. Ratajczak. *J. Mol. Struct.* 656 (2003) 275.
- [18] S. Zheng, Y. L. Mi. *Polymer* 44 (2003) 1067.
- [19] Y. H. Liang, C.C. Wang, C.Y. Chen, *European Polymer Journal* 44 (2008) 2376.
- [20] Z.C. Zhang, L. J. Lyons, K. Amine, R. West, *Macromolecules* 38 (2005) 5714.
- [21] J. Zhao, Y. Ishigaki, M. Yamanaka, H. Fukuda, K. Aoi, *J. Power Sources* 189 (2009) 359.
- [22] Y. Masuda, M. Seki, M. Nakayama, M. Wakihara., H. Mita, *Solid State Ionics* 177 (2006) 843.
- [23] K. Amine, Q. Z. Wang, D. R. Vissers, Z.C. Zhang, N. A.A. Rossi, R. West, *Electrochem. Commun.* 8 (2006) 429.
- [24] Y. Kang, H. J. Kim, E. Kim, B. Oh, J. H. Cho, *J. Power Sources* 92 (2001) 255.
- [25] A. Bac, M. Ciosek, M. Bukat, M. Marczewski, H. Marczewska, W. Wiczcerek, *J. Power Sources* 159 (2006) 405.

Figure Captions



a MPEGM



b HPEGM

Fig. 1. Chemical structures of MPEGM and HPEGM macro-monomers.

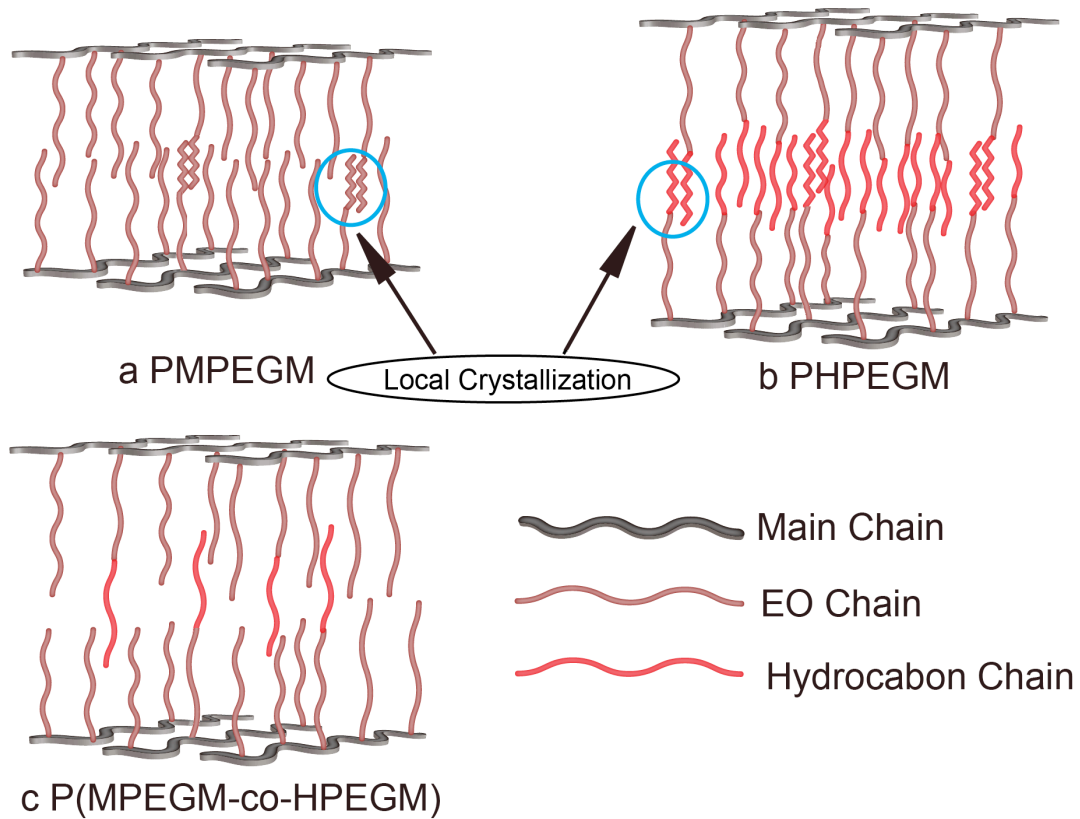


Fig. 2. Schematic illustrations for the ideal structure of (a) PMPEGM, (b) PHPEGM and (c) P(MPEGM-co-HPEGM)

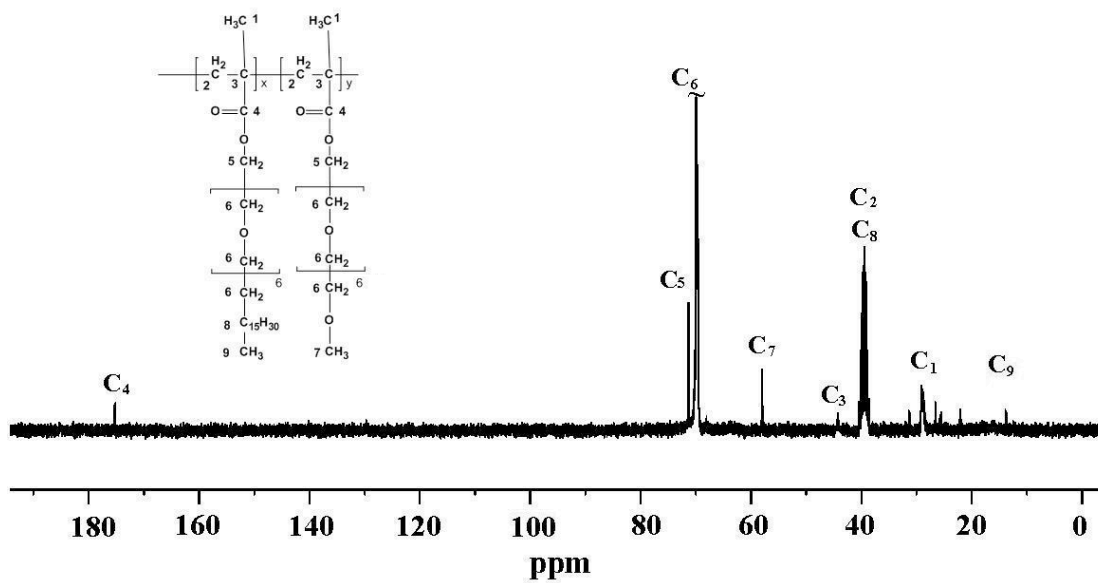


Fig.3 ^{13}C -NMR spectrum of PMH₇₋₈₀.

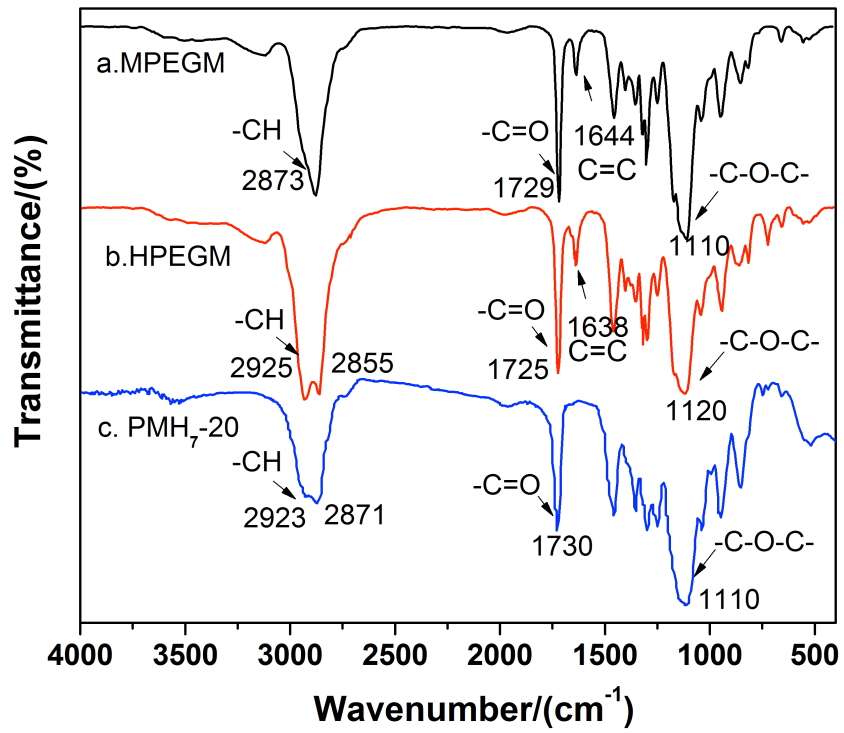


Fig. 4. IR spectrum of MPEGM (n=7), HPEGM and PMH₇-80.

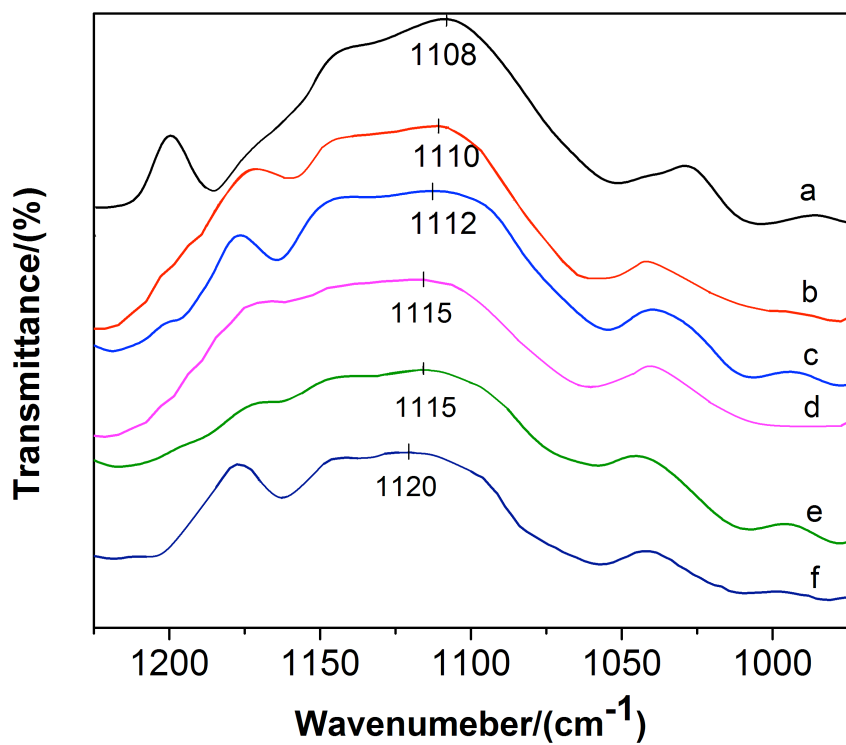


Fig. 5. IR spectra of C–O–C groups of different polyethylene glycol derivatives and chemical structures of the derivatives are shown in Table 1.

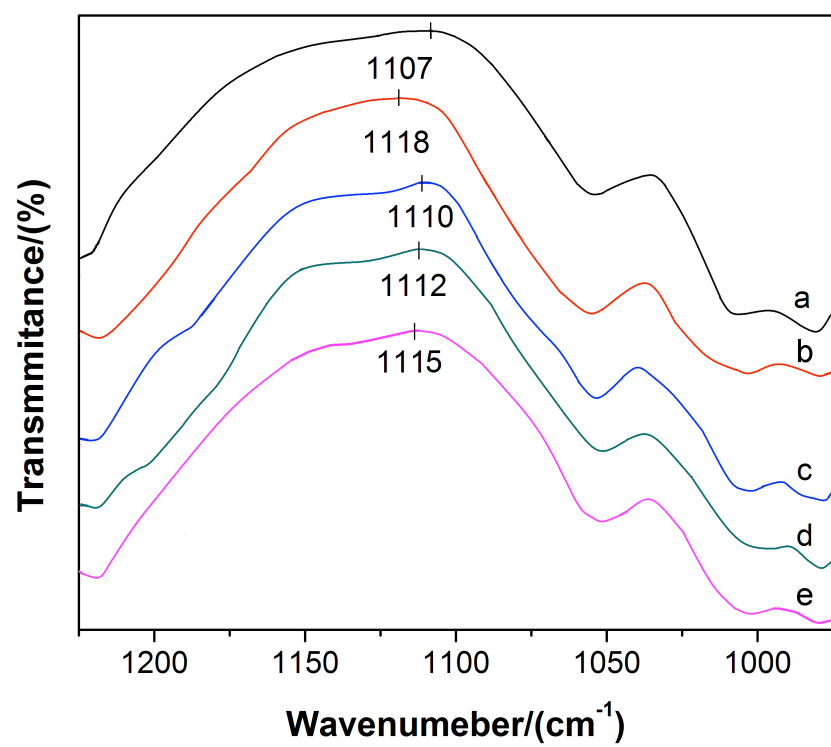


Fig.6. IR spectra of C–O–C groups in polymers. (a) PMPEGM (n=7), (b) PHPEGM, (c) PMH₇-80, (d) PMH₇-60, (e) PMH₇-40.

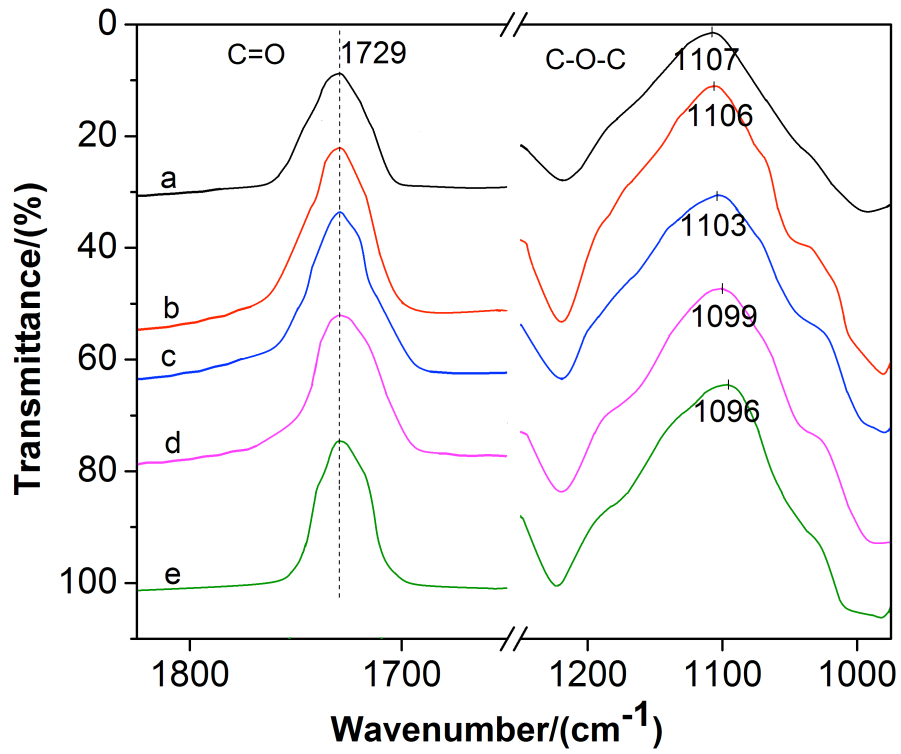


Fig.7. IR spectra of C–O–C and C=O group in electrolytes. (a) PMH₇-80 ([Li]:[EO] =1:30), (b) PMH₇-80 ([Li]:[EO] =1:25), (c) PMH₇-80 ([Li]:[EO] =1:20), (d) PMH₇-80 ([Li]:[EO] =1:15), (e) PMH₇-80 ([Li]:[EO] =1:10).

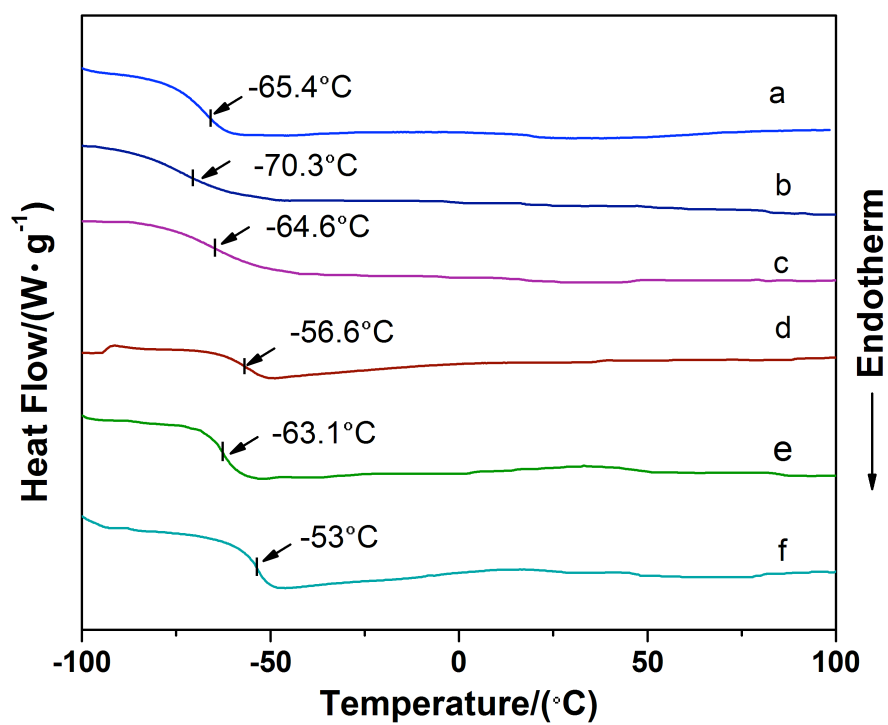


Fig. 8. DSC traces for the polymers and electrolytes. (a) PMH₇₋₈₀ (b) PMH₁₂₋₇₅ (c) PMH₁₆₋₇₀ (d) PMH₇₋₈₀ ([Li]:[EO] = 1:20), (e) PMH₁₂₋₇₅ ([Li]:[EO] = 1:20), (f) PMH₁₆₋₇₀ ([Li]:[EO] = 1:20).

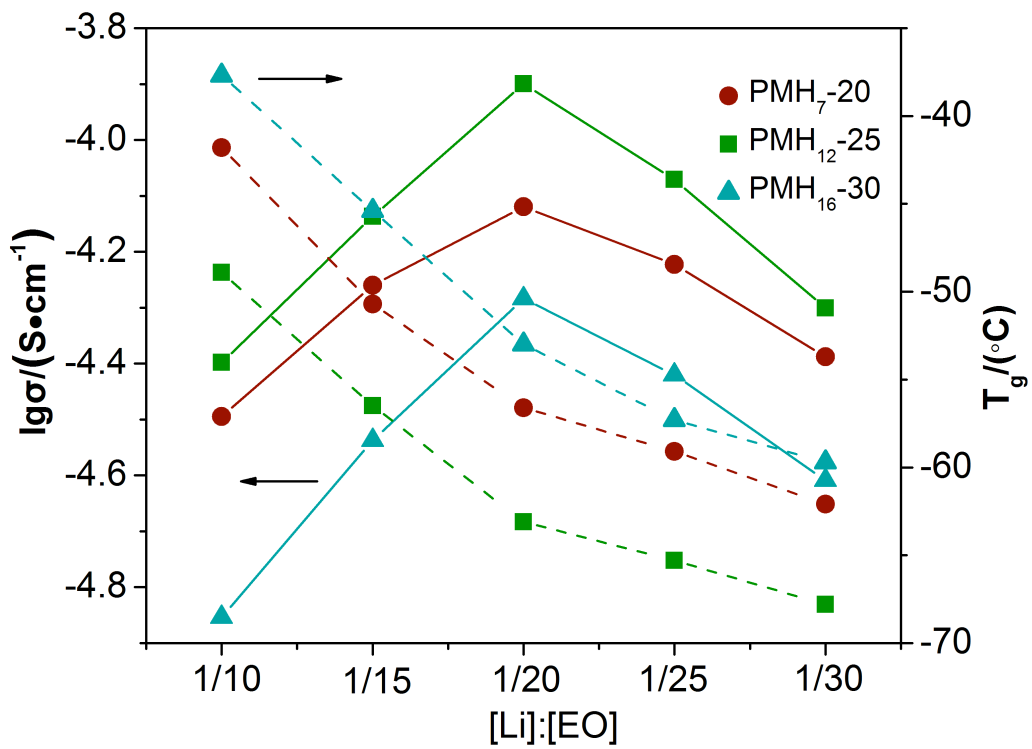


Fig. 9. The dependence of the ionic conductivity and T_g on the [Li]:[EO] ratio.

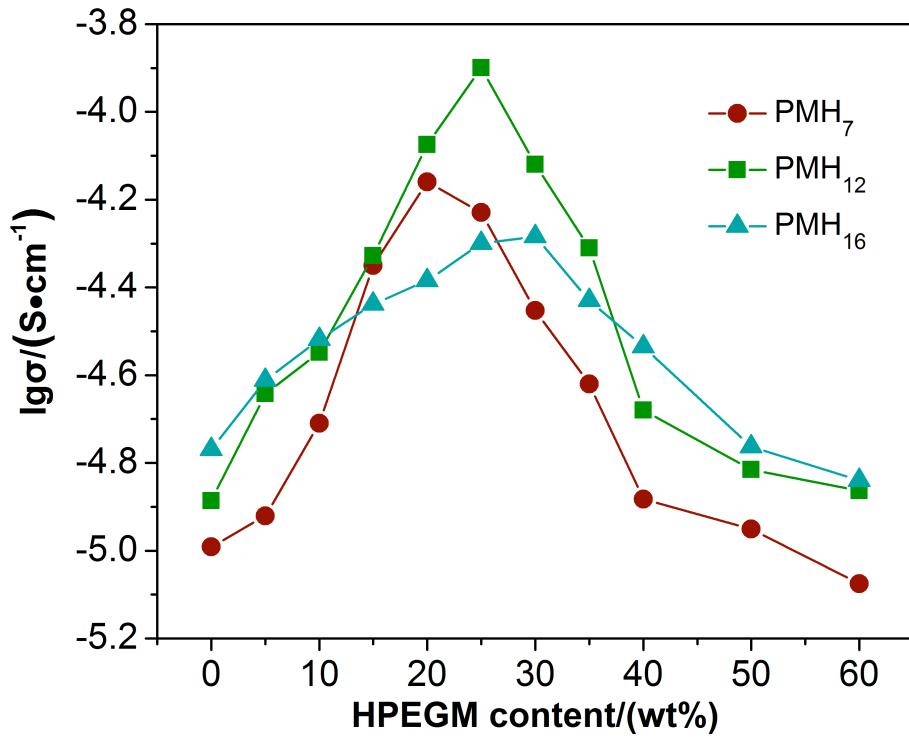


Fig. 10. The conductivity of the electrolytes with various number of repeat units in MPEGM are measured as a function of HPEGM content.

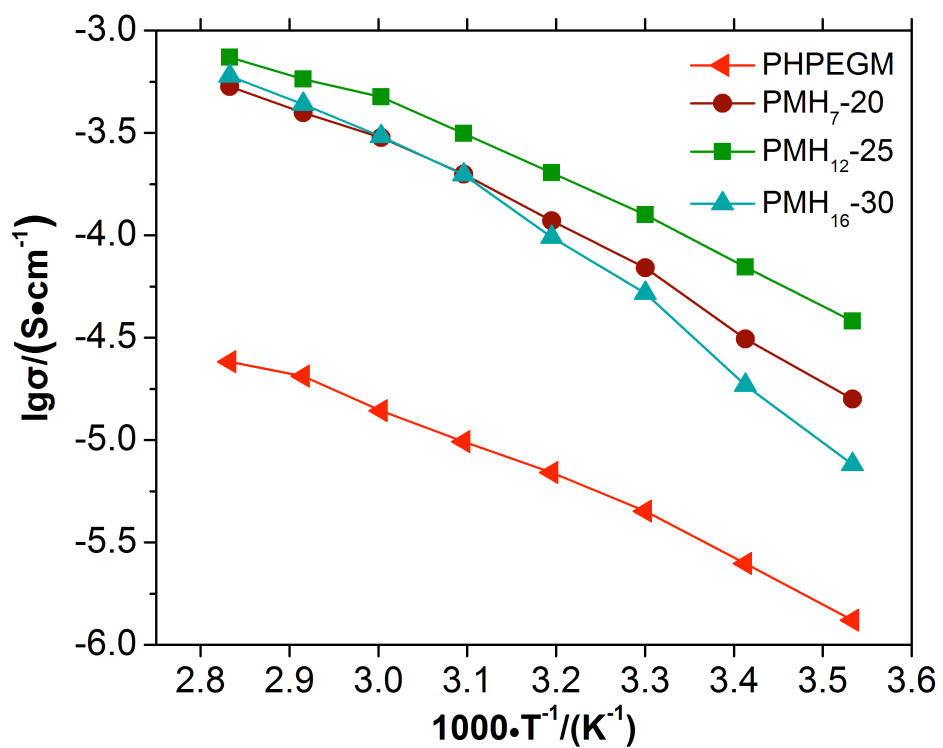


Fig. 11. shows the cyclic voltammograms of the electrolytes with various number of repeating units of EO in the MPEGM on Ni working electrode and Li counter/reference electrode swept from (a) $-0.5V$ to $2.5 V$ vs. Li^+/Li and (b) $2.5V$ to $5.5 V$ vs. Li^+/Li at $30^{\circ}C$.

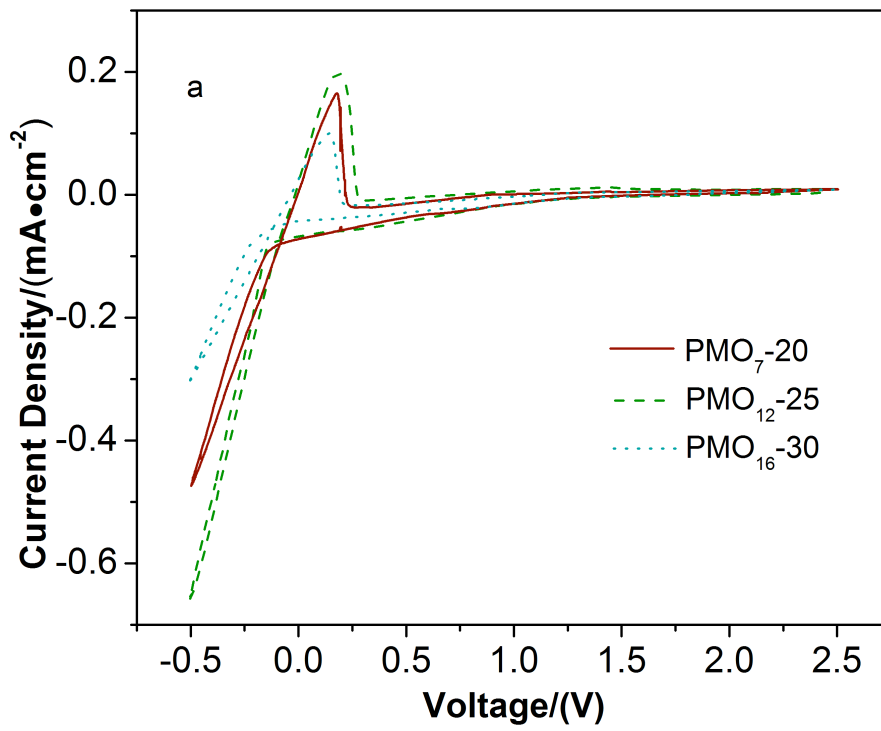
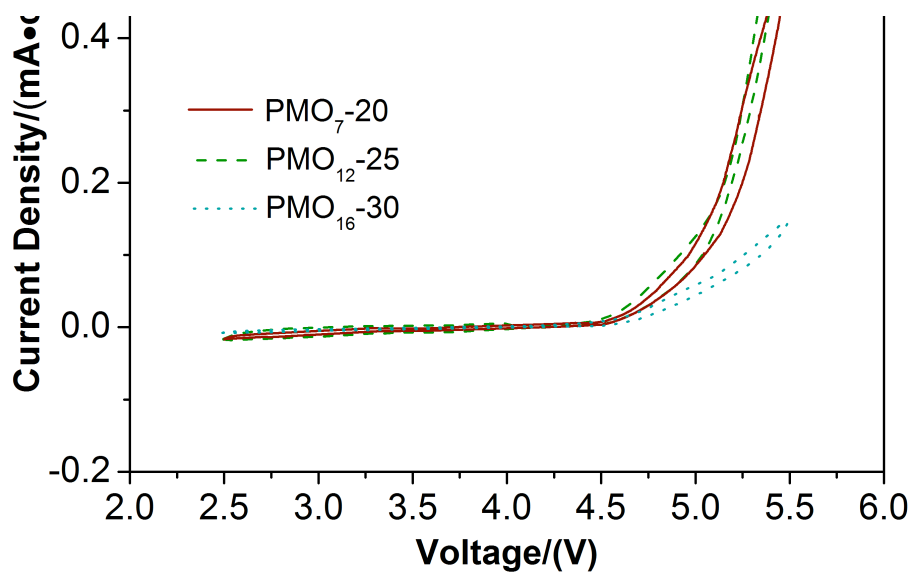


Fig. 12. (a) Impedance profiles of Li/PMH₁₂-75 ([Li]:[EO] =1:20)/SS; (b) Time dependence profiles of the bulk and interfacial resistances.

Table 1. Chemical structures of polyethylene glycol derivatives in Fig. 2.

No.	Chemical Structure	NO.	Chemical Structure
a	$\text{H}_3\text{C} \left[\text{O}-\overset{\text{H}_2}{\text{C}}-\overset{\text{H}_2}{\text{C}} \right]_7 \text{OCH}_3$	d	$\text{H}_3\text{C} \left[\text{O}-\overset{\text{H}_2}{\text{C}}-\overset{\text{H}_2}{\text{C}} \right]_7 \text{O}-\overset{\text{O}}{\parallel}{\text{C}}-\text{C}_{11}\text{H}_{23}$
b	$\text{H}_3\text{C} \left[\text{O}-\overset{\text{H}_2}{\text{C}}-\overset{\text{H}_2}{\text{C}} \right]_7 \text{O}-\overset{\text{O}}{\parallel}{\text{C}}-\text{C}_7\text{H}_{15}$	e	$\text{C}_7\text{H}_{15}-\overset{\text{O}}{\parallel}{\text{C}}-\text{O} \left[\overset{\text{H}_2}{\text{C}}-\overset{\text{H}_2}{\text{C}}-\text{O} \right]_7 \overset{\text{O}}{\parallel}{\text{C}}-\text{C}_7\text{H}_{15}$
c	$\text{H}_3\text{C} \left[\text{O}-\overset{\text{H}_2}{\text{C}}-\overset{\text{H}_2}{\text{C}} \right]_7 \text{O}-\overset{\text{O}}{\parallel}{\text{C}}-\text{C}(\text{C}_2\text{H}_5)\text{C}_4\text{H}_{10}$	f	$\text{C}_4\text{H}_{10}(\text{C}_2\text{H}_5)\text{C}-\overset{\text{O}}{\parallel}{\text{C}}-\text{O} \left[\overset{\text{H}_2}{\text{C}}-\overset{\text{H}_2}{\text{C}}-\text{O} \right]_7 \overset{\text{O}}{\parallel}{\text{C}}-\text{C}(\text{C}_2\text{H}_5)\text{C}_4\text{H}_{10}$

Table 2. Thermal data and conductivity of polymers and electrolytes

Sample	T _g (°C)	T _c (°C)	ΔH _c (J·g ⁻¹)	T _m (°C)	ΔH _m (J·g ⁻¹)	σ (S·cm ⁻¹) at 30°C
PMPEGM(n=7)	-54.7	-	-	8.4	6.2	
PMPEGM(n=12)	-55.3	-16.3	19.7	18.9	37.2	
PMPEGM(n=16)	-59.5	-7.6	20.4	33.8	53.6	
PHPEGM	-79.7	-8.2	20.7	-	-	
PMH ₇ -80	-65.4	-	-	-	-	
PMH ₁₂ -75	-70.3	-	-	-	-	
PMH ₁₆ -70	-64.6	-	-	-	-	
PHPEGM	-72.5	-10.1	11.9	-	-	4.47×10 ⁻⁶
[Li]/[O] = 1:20						
PMH ₇ -80	-56.6	-	-	-	-	7.6×10 ⁻⁵
[Li]/[O] = 1:20						
PMH ₁₂ -75	-63.1	-	-	-	-	1.26×10 ⁻⁴
[Li]/[O] = 1:20						
PMH ₁₆ -70	-53.0	-	-	-	-	5.2×10 ⁻⁵
[Li]/[O] = 1:20						

Table 3. VTF fitting parameters for electrolytes

Sample	A ($\text{S} \cdot \text{K}^{1/2} \cdot \text{cm}^{-1}$)	E_0 ($\text{kJ} \cdot \text{mol}^{-1}$)	T_0 (K)	T_g (K)
PHPEGM	0.051	7.26	150.5	200.5
[Li]:[EO] = 1:20				
PMH ₇ -80	2.62	8.63	166.4	216.4
[Li]:[EO] = 1:20				
PMH ₁₂ -75	2.23	8.12	159.9	209.9
[Li]:[EO] = 1:20				
PMH ₁₆ -70	3.89	8.90	170.0	220.0
[Li]:[EO] = 1:20				